Journal of Materials Chemistry A

PAPER

View Article Online
View Journal | View Issue

# V-substituted $In_2S_3$: an intermediate band material with photocatalytic activity in the whole visible light range

Cite this: J. Mater. Chem. A, 2014, 2, 8236

Raquel Lucena,[a] José C. Conesa,*[a] Irene Aguilera,†[bc] Pablo Palacios[bd] and Perla Wahnón[bc]

We proposed in our previous work V-substituted $In_2S_3$ as an intermediate band (IB) material able to enhance the efficiency of photovoltaic cells by combining two photons to achieve a higher energy electron excitation, much like natural photosynthesis. Here this hyper-doped material is tested in a photocatalytic reaction using wavelength-controlled light. The results evidence its ability to use photons with wavelengths of up to 750 nm, *i.e.* with energy significantly lower than the bandgap (=2.0 eV) of non-substituted $In_2S_3$, driving with them the photocatalytic reaction at rates comparable to those of non-substituted $In_2S_3$ in its photoactivity range ($\lambda \leq 650$ nm). Photoluminescence spectra evidence that the same bandgap excitation as in V-free $In_2S_3$ occurs in V-substituted $In_2S_3$ upon illumination with photons in the same sub-bandgap energy range which is effective in photocatalysis, and its linear dependence on light intensity proves that this is not due to a nonlinear optical property. This evidences for the first time that a two-photon process can be active in photocatalysis in a single-phase material. Quantum calculations using GW-type many-body perturbation theory suggest that the new band introduced in the $In_2S_3$ gap by V insertion is located closer to the conduction band than to the valence band, so that hot carriers produced by the two-photon process would be of electron type; they also show that the absorption coefficients of both transitions involving the IB are of significant and similar magnitude. The results imply that V-substituted $In_2S_3$, besides being photocatalytically active in the whole visible light range (a property which could be used for the production of solar fuels), could make possible photovoltaic cells of improved efficiency.

Received 28th January 2014
Accepted 19th March 2014

DOI: 10.1039/c4ta00513a

www.rsc.org/MaterialsA

## Introduction

Making the most effective use of solar light, by converting with good efficiency the widest range of the spectrum, is a requirement in both photocatalytic and photovoltaic applications. In photovoltaic (PV) technology, apart from the use of tandem cells,[1] in which several different semiconductors absorbing photons of different energies are stacked on top of one another, one proposed way of achieving that objective is based on the intermediate band (also called multiband or impurity photovoltaic) scheme, first formulated by Wolf[2] and which received later strong momentum after the work by Luque and Martí.[3] In this system (see Fig. 1) the excitation of one electron from the valence band (VB) of a semiconductor to its conduction band (CB) across the separation between the two bands (the bandgap) can be achieved not only upon absorption of one photon having

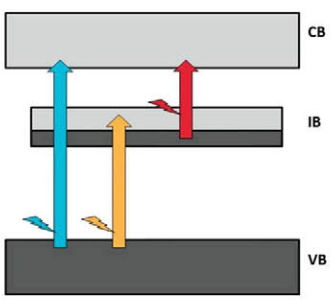


Fig. 1 Scheme of the intermediate band working principle, in which the successive absorption of two lower energy photons can drive a higher energy electron excitation, like in a higher energy photon absorption.

[a]Instituto de Catálisis y Petroleoquímica, CSIC, Marie Curie 2, Campus de Excelencia UAM-CSIC, 28049 Madrid, Spain. E-mail: jcconesa@icp.csic.es; rlucena@icp.csic.es; Fax: +34-915854760; Tel: +34-915854766

[b]Grupo de Cálculos Cuánticos (Unidad Asociada al Instituto de Catálisis y Petroleoquímica, CSIC), Instituto de Energía Solar, Univ. Politécnica de Madrid, Avda. Complutense 30, 28040 Madrid, Spain

[c]Dpt. TEAT, E.T.S. de Ingenieros de Telecomunicación, Univ. Politécnica de Madrid, Avda. Complutense 30, 28040 Madrid, Spain. E-mail: perla@etsit.upm.es

[d]Dpt. FyQATA, EUIT Aeronáutica, Univ. Politécnica de Madrid, Ciudad Universitaria, 28040 Madrid, Spain. E-mail: pablo.palacios@upm.es

† Present address: Peter Grünberg Institut and Institute for Advanced Simulation, Forschungszentrum Jülich, D-52425 Jülich, Germany, E-mail: i.aguilera@fz-juelich.de.

energy higher than the bandgap width $E_g$, but also upon absorption of two lower energy photons which respectively promote the electron from the VB to an additional narrow band (the intermediate band, IB) located between the VB and the CB and from the IB to the CB. A higher current can thus be collected in a PV cell while maintaining the voltage corresponding to the energy difference between the VB and CB. According to the calculations in ref. 3 the maximum ideal efficiency that can be obtained with a so built PV cell is more than 1.5 times higher than that achievable with a normal single-gap semiconductor. Such maximum increased efficiency may result in an overall bandgap $E_g = 1.95$ eV and a partition of it by the IB in two sub-bandgaps of about 1.25 and 0.7 eV respectively, the effect being the same if the VB–IB partial gap is the smaller or the larger one.

Implementing this two-photon working principle and verifying its usefulness in photocatalysis (and eventually in photovoltaic devices as well) is the objective of the present work. Actually, in photocatalysis the idea of enlarging the spectral response of a wide band gap semiconductor, and especially of one of the paradigmatic photocatalysts $TiO_2$ and ZnO, through insertion (*via* doping) of additional levels in the band gap is several decades old.[4] In contrast to the IB scheme, however, that idea does not consider in general the possibility of coupling two photons in one same (monophasic) material, but just tries to achieve an effective decrease in $E_g$. Coupling two photons for photocatalysis is considered mainly in systems where two semiconductors are in intimate contact or linked by an electron shuttle so that after the absorption of photons in both of them electrons photogenerated in one of them neutralize holes photoproduced in the other one, leading to a better charge separation and possibly higher overall chemical potential. A similar coupling of the absorption of two photons in different absorbers to achieve a higher energy electron excitation is used in natural photosynthesis, which operates through the so-called Z-scheme.[5] At difference with nature and with the mentioned two-phase approach, the IB scheme discussed here does not separate spatially both absorptions, so that a smaller number of electron transfer barriers exists, having in addition the advantage of making possible the full electronic transition also using only one (higher energy) photon.

Apart from systems based on quantum dots,[6] one way to achieve the IB PV scheme is the introduction of the IB levels in a parent semiconductor *via* (hyper) doping. This should be done at a concentration high enough such that the levels inserted have a delocalized character, forming a true band; this has been shown to reduce nonradiative recombination.[7] A higher concentration will also increase the absorption coefficients of the sub-bandgap transitions, which in quantum dot-based systems are rather weak. In the past few years we have proposed, based on solid state chemistry concepts and quantum mechanical calculations, several materials of this kind in which a transition metal (TM) is used as a dopant: Ti-substituted III–V semiconductors,[8] Ti- and Cr-substituted $CuGaS_2$ chalcopyrite[9] and $SnS_2$ and indium thiospinels (like $In_2S_3$ or $MgIn_2S_4$) in which the octahedral cation is partially substituted by vanadium,[10,11] these latter systems having been realized experimentally.[10,12] Other substituted systems experimentally achieved and claimed to constitute as well IB materials are highly mismatched alloys, assumed to form the IB through a band anticrossing effect[13,14] (although in these reports it was not always clear whether the partial filling condition is fulfilled to the necessary extent); Cr-substituted GaN, where spectra and photovoltaic response seem to agree with the claimed IB structure[15] although the bandgap of the GaN host compound, 3.4 eV, is rather higher than the optimum value for efficient IB PV cell operation; Nb-substituted $In_2S_3$, for which the IB character is inferred from optical and opto-electronic properties;[16] Cr- or Sn-substituted $CuGaS_2$, where it has been claimed that the IB principle operates in photocatalytic reactions;[17] or Fe-substituted In thiospinels which show optical spectra agreeing with the IB characteristics predicted by DFT calculations.[18] Note also that Mn-substituted GaAs or GaP, studied intensely in the last few years for their interest in spintronics, may have also a partially filled IB.[19]

Concerning photocatalysts, as said above many attempts (besides the two substituted $CuGaS_2$ materials just mentioned) to obtain a wider spectral response *via* doping have been made, although the efficiency of the sub-bandgap energy photons absorbed is usually found to be much lower than that obtained with absorbed photons in the corresponding non-substituted material. This is generally ascribed to recombination processes induced by the dopant, the electronic levels of which will be localized if the dopant concentration is not high enough. The low mobility of the charge carriers formed on these dopants may be also a relevant factor for this, especially when the dopant is a transition metal which will have rather localized orbitals.

The mentioned work of ours on V-substituted $SnS_2$[10] showed experimentally with the aid of a photocatalytic reaction that this material can produce electron–hole pairs when irradiated with photons of energy lower than the $SnS_2$ bandgap ($\approx$2.2 eV[20]). In the present article a similar procedure is used to show that the previously prepared and reported V-substituted $In_2S_3$[12] can also sustain photocatalysis with photons of energy lower than the bandgap of pure $In_2S_3$ ($\approx$2.0 eV,[21] *i.e.* very close to the optimum one for the IB scheme), which confirms as well its IB material characteristics and thus its validity not only for photocatalytic processes using the full visible light range but also for making an IB PV device. The formation of CB electrons and VB holes through this coupling of two sub-bandgap energy photons is evidenced as well with photoluminescence experiments. We also present many-body (GW-type) calculations confirming the formation of the IB band within the semiconductor bandgap as was proposed previously[11] using standard density functional theory (DFT). For V-substituted $In_2S_3$ full GW calculations are computationally too demanding, so calculations have been made for $MgIn_2S_4$ (having also a thiospinel structure and overall properties close to those of $In_2S_3$ but a smaller number of atoms in the primitive unit cell: 14 *vs.* 40), also substituted with V. In these GW calculations the gap between VB and IB appears enlarged compared to the LDA results, as was also observed in other proposed IB systems such as the $Cu_4CrGa_3S_8$ chalcopyrite[22] and the inverse spinel $Mg_2TiIn_3S_8$.[23] Therefore this GW

effect of VB to IB gap enlargement can probably be extended to other IB materials in addition to the V:$In_2S_3$ studied here.

In the context of the present work it is worth mentioning that, while $TiO_2$ is the material most usually considered for photocatalysis and a number of other materials have been assayed for photocatalysis,[24] $In_2S_3$ has been considered previously as a photocatalyst by a significant but smaller number of other authors.[25] As a procedure to improve the spectral response of a photocatalyst, doping of the latter (among other methods[26]) is frequently considered, particularly in the case of $TiO_2$, but normally the aim is just a decrease in the bandgap, not allowing a two-photon process, in order to make the material visible light-responsive,[27] and in any case this has not been tried for $In_2S_3$ by other groups; the above mentioned work by Ho[16] is only concerned with photovoltaic behaviour. Note, finally, that an improvement in photocatalytic efficiency can be obtained also *via* coupling to another material which may help separating electrons and holes; this has been done occasionally with $In_2S_3$ itself.[28] The possibility of doing it with the V-substituted material studied in this work is not addressed here.

# Materials and methods

### Experimental procedures

The synthesis and characterization of $In_2S_3$ polycrystalline powder (with or without V in it) through a solvothermal reaction at 463 K, using $InCl_3$, $VCl_3$ and $Na_2S$ as reagents, was reported previously.[12] It was verified there that the V-containing product, with a V : In ratio = 1 : 10.7, displayed in the XRD pattern only the features of pure $In_2S_3$ with an average nanocrystallite size of $\approx$20 nm very similar to that of the similarly prepared V-free $In_2S_3$, with no hint of an additional V-related phase or amorphous component. HRTEM-EDS analysis showed a V : In ratio close to the bulk composition also in regions of the sample containing only a single crystallite of the indium thiospinel phase, confirming thus the presence of V in the $In_2S_3$ lattice (see the ESI of ref. 12). As shown also in ref. 12 the UV-vis-NIR spectrum of this material displayed, in comparison with that of V-free $In_2S_3$ (which indicated a bandgap of ~2.1 eV), new light absorption features in the sub-bandgap range, appropriate for the IB electronic structure which had been predicted for this system by DFT calculations. The specific surface of that sample, which was measured but omitted in that paper, is 28.5 $m^2\ g^{-1}$, thus of the same order as the 40 $m^2\ g^{-1}$ value measured for the V-free sample and reported in ref. 11.

The photocatalytic reaction test setup and procedure has been described previously as well.[10] It consists of a pyrex glass photoreactor in which a stirred and aerated suspension of the sulphide powder at 0.5 $g\ L^{-1}$ concentration in a 1.5 mM solution of HCOOH, phosphate-buffered at pH = 2.5, is irradiated with light from a 400 W ozone-free Xe lamp, filtered through pure water to suppress most of the thermal IR part; the intensity of the polychromatic light beam incident on the liquid surface is *ca.* 175 mW $cm^{-2}$. To this lamp optical bandpass filters can be fitted that select a relatively narrow wavelength range (FWHM $\approx$ 50 nm) around a chosen central value. The reaction of HCOOH is monitored by periodic sampling of suspension aliquots, filtration and UV spectrometric measurement of the remaining HCOOH concentration in the liquid through its absorbance at $\lambda$ = 205 nm.

Photoluminescence tests at ambient temperature were carried out using a Perkin-Elmer LS50B fluorimeter with monochromatized excitation light. In the experiments using a fixed wavelength of exciting light, the latter was additionally filtered with an appropriate filter to ensure that no wavelengths from higher order diffractions reached the sample.

### Calculation methods

Local density approximation (LDA–DFT) and many-body calculations were carried out using the ABINIT code[29,30] with norm-conserving pseudopotentials generated through the *fhi98PP* code.[31] Semicore states (*i.e.*, 4s, 4p, 4d for In and 3s, 3p for V) were taken into account explicitly in the valence levels manifold because it is known that this may substantially affect results for GW calculations.[32] LDA results were used as the starting point for a self-consistent Coulomb-hole and screened-exchange (COHSEX)[33] calculation, and the results of the latter were then used for a dynamic $G_0W_0$ step. A basis set of around 30 000 plane waves was required for convergence of the COHSEX and $G_0W_0$ calculations. A Monkhorst–Pack $k$-point mesh of 3 × 3 × 3 was used to sample the Brillouin zone (BZ), which corresponds to 14 k points in the irreducible BZ. GW corrections were interpolated using a quadratic interpolation for the denser $k$-mesh needed for the calculation of optical properties and density of states. For $G_0W_0$ calculations the plasmon-pole model[34] was adopted and 400 bands were taken into account. They were carried out after a LDA relaxation of cell and ion positions, which led to a lattice parameter of 10.47 Å. The dielectric function was obtained using ABINIT within the random phase approximation (RPA), using the sc-COHSEX + $G_0W_0$ eigenvalues and the LDA wavefunctions and neglecting local-field effects in the calculation of the macroscopic average. The absorption coefficient was obtained from the real and imaginary parts of the dielectric function.[35]

# Results and discussion

### Photocatalytic test results

As reported earlier,[36] the V-free $In_2S_3$ powder can sustain the photo-degradation of HCOOH in aqueous suspension if irradiated with photons having energy around or above its 2.0 eV bandgap, *i.e.* with $\lambda \leq$ 650 nm (see Fig. 2a). The photocatalyst was verified in that work to be more stable against photocorrosion in this process than the much used CdS material; in fact, $In_2S_3$ has been verified to be stable as a photocatalyst in the presence of electron-donor compounds.[25h] The overall process can be assumed to consist of a simple total oxidation:

$$HCOOH + 1/2O_2 \rightarrow CO_2 + H_2O$$

initiated by electrons and holes photo-generated in the semiconductor, which diffuse into the solid–liquid interface and are transferred there to adsorbed $O_2$ molecules (dissolved in the

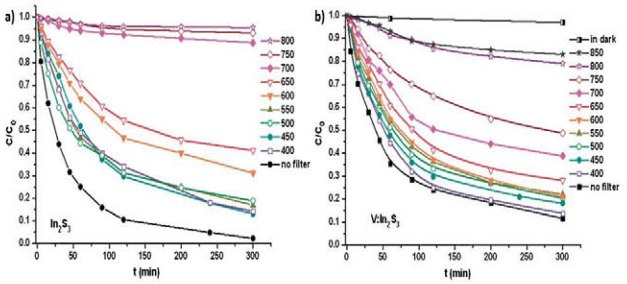


Fig. 2 HCOOH concentration decay upon irradiation with light of different wavelengths in aqueous suspensions with $In_2S_3$ (a) and V:$In_2S_3$ (b). The error in the concentration measurements, as judged from repeated tests, is *ca.* 5% of the initial concentration.

liquid from air) and $H_2O$ or surface $OH^-$ groups respectively, giving in these processes $O_2^-$ or OH˙ radicals:

$$h\nu \rightarrow h^+ + e^-$$

$$e^- + O_2 \rightarrow O_2^-$$

$$h^+ + OH^- \rightarrow OH^{\cdot} \text{ (or } h^+ + H_2O \rightarrow OH^{\cdot} + H^+)$$

These very reactive species further evolve and attack HCOOH present at or near the surface, presumably by hydrogen abstraction steps, as could be for example

$$OH^{\cdot} + HCOOH \rightarrow {}^{\cdot}COOH + H_2O$$

$$O_2^- + {}^{\cdot}COOH \rightarrow CO_2 + HO_2^-$$

Other reactions involving these radicals as well as the peroxidic $HO_2^-$ species, not discussed in detail in this work, may take place to produce the final $CO_2$ and $H_2O$ products; the details of the reaction mechanisms are not dealt with here. In principle one could consider also other photon-induced overall reactions leading to different decay products like CO, $H_2$ or oxalic acid:

$$HCOOH \rightarrow CO + H_2O$$

$$HCOOH \rightarrow CO_2 + H_2$$

$$2HCOOH + 1/2O_2 \rightarrow (COOH)_2 + H_2O$$

The first reaction is usually catalyzed by acidic solids, and is unlikely to occur here since $In_2S_3$ is a rather basic compound; the second one would require an efficient catalyst of H–H bond formation (like Pt or Ni) and the third one can be discarded since when the reaction was carried out in unbuffered solution the pH was observed to rise and reach near-neutral conditions, which would not be the case if oxalic acid were formed.

The process was repeated with the V:$In_2S_3$ material. Under irradiation the HCOOH concentration in the aqueous suspension was found to decrease gradually, doing so at different rates depending on the wavelength of the filtered light used. Fig. 2 displays the concentration decrease determined for different wavelengths, compared with that found previously for V-free $In_2S_3$.[36] Fig. 2 also includes the results obtained with unfiltered light (note that for all curves the experiment was started with a fresh portion of the sulphide powder). It can be seen that for a range of wavelengths corresponding to photon energies clearly below the $In_2S_3$ bandgap width (between 700 and 750 nm) the decrease is much faster for the V-containing photocatalyst. Semilogarithmic plots (not shown) verified that these decay curves follow approximately a (pseudo) first order kinetics:

$$C(t) = C_0 e^{-kt}$$

This allows quantifying the effect through the rate constant $k$, obtained from a fit to the initial curve slope. When the irradiation was carried out with the full unfiltered light from the Xe lamp a value $k = 0.014$ min$^{-1}$ was obtained for the V-substituted $In_2S_3$ material; this can be compared with the value $k = 0.018$ min$^{-1}$ determined for the V-free sample, which shows that the insertion of V in the sulphide structure does not impair too much the overall photocatalytic efficiency. The results obtained with filtered light can be summarized plotting the value of $k$ as a function of the filter wavelength $\lambda$; this is shown in Fig. 3, where again the data obtained for V-free and V-containing $In_2S_3$ are compared, and which includes also the UV-vis-NIR spectra of these materials in the displayed range.

The main effect of adding V is clearly seen to consist in a significant extension of the wavelength range in which the photocatalytic process can take place. Thus for V-free $In_2S_3$ photocatalytic activity is observed with $\lambda$ up to 650 nm (a wavelength somewhat above the value $\lambda = 620$ nm which corresponds to $E_g = 2.0$ eV; this somewhat extended range can be ascribed to the combination of the small tail seen in the absorption spectrum in this range and the width of the wavelength band transmitted by the filters), while for the V-containing material the photocatalytic reaction is detected for $\lambda$ up to 750 nm, *i.e.* the action spectrum extends to the beginning of the IR range. This means that the substituted sample acts as

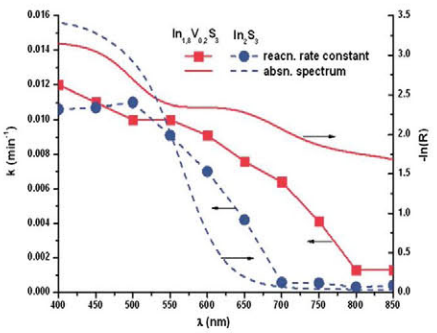


Fig. 3 Reaction rate constant $k$ of the photocatalytic HCOOH degradation plotted against light wavelength for $In_2S_3$ and V:$In_2S_3$. The optical spectrum of both materials (shown as the logarithm of diffuse reflectance), already given in ref. 12, is superimposed on these curves.

having an effective bandgap around 1.65 eV (which corresponds to a wavelength of 750 nm), smaller than that of pure $In_2S_3$; indeed the wavelength range extension parallels the extension in the absorption range indicated by the step which appears starting at $\lambda \approx 750$ nm in the spectrum of V-free $In_2S_3$. Here one may note that Fig. 3 would imply that, if all wavelengths were included, the total reaction rate should be larger for the V-substituted sample, contrarily to the observation mentioned above. This apparent contradiction may be due to the much higher light intensity in the unfiltered case, indeed significantly higher than normal solar light intensity, which is about 100 mW $cm^{-2}$ including the thermal IR component; therefore the effect may be smaller under solar irradiation. This may produce a proportionally higher level of nonradiative recombination (the latter normally scales with the product of electron and hole concentrations, *i.e.* with the square of the light intensity) which at this intensity level might be more enhanced in the presence of vanadium. Or it may be due to a different rate of the two sub-bandgap electron transitions involving the IB, which for high light intensity might lead to a significant change in the degree of filling by electrons in the IB, altering the efficiency of the two-photon process. With the present data it is not possible to ascertain between these two mechanisms. Apart from this, some minor effects like the not exact parallel between the differences in the absorption spectrum and in the photocatalytic activity of both samples might be due to small differences between these in the dynamics and transport of the carriers photoexcited with different wavelengths.

It is worth noting that the fact that very similar reaction rates are obtained in both materials when using photons with energy well above the bandgap of $In_2S_3$ (*i.e.* $\lambda < 600$ nm) implies that the introduced V ions do not contribute much to increase electron–hole recombination, meaning that the new levels introduced do have the desired delocalized character which as said above allows minimizing nonradiative recombination. Furthermore, the rate constant observed for the V-containing material in the wavelength range approaching its effective bandgap (*i.e.* around 700–750 nm) is close to that obtained for pure $In_2S_3$ in the range approaching its own bandgap (*i.e.* 600–650 nm), which implies that the mobility and transferability (to the dissolved reactants) of the charge carriers photogenerated with sub-bandgap photons in the former material are similar to those of typical photogenerated electrons and holes in the latter one. This makes unlikely the alternative explanation that could be proposed for the observed effect, based on assuming that it could be due to just a one-electron excitation between the IB levels and the CB or the VB, *i.e.* to a mere reduction of the effective bandgap. If it were so, one would expect a much reduced effectiveness of the generated charge carriers, due to both the lower mobility expected for the states in the IB and the smaller redox potential that would be available.

To get further insight into the mechanism of the photon-induced chemistry the formation of $OH^{\bullet}$ radicals, which may be the first step in the action of photogenerated holes, was monitored with terephthalic acid. This molecule is known[37] to scavenge $OH^{\bullet}$ radicals in aqueous solution to give hydroxy-terephthalic acid, detectable through its violet fluorescence under UV light:

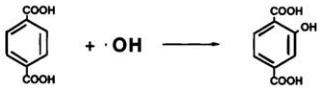


Thus a test was made, similar to that on HCOOH and using the same setup but with 1.0 mM terephthalic acid. The formation of the hydroxyl derivative was detected with the fluorimeter (Fig. 4a), and the fluorescence intensity generated upon irradiation with different wavelengths was plotted against time for both $In_2S_3$ and V:$In_2S_3$ samples (Fig. 4b and c). It can be seen again that comparable photoreaction rates are obtained for both materials when irradiating with photons having energy above the $In_2S_3$ bandgap, while irradiation with 700 nm photons gives significant reaction only for the V-containing sample and negligible products are obtained with 800 nm photons. This shows that the two-photon process made possible by the intermediate band is indeed able to produce $OH^{\bullet}$ radicals active in photocatalytic reactions.

## Photoluminescence tests

Fig. 5 presents the spectra of emitted light obtained for both $In_2S_3$ and V:$In_2S_3$ samples when excited by monochromatic light of different wavelengths. When using for the excitation photons of wavelengths below 550 nm both samples show a weak but distinct emission at *ca.* 595 nm (photon energy $\approx$2.1 eV, *i.e.* close to $E_g$), which has been observed in the literature for single-crystal or powdered $In_2S_3$ at both ambient and cryogenic temperatures[38,39] and is ascribed to the recombination of charge carriers at the VB and CB edges. One significant result here is that the intensity emitted when irradiating with photons having energy above the $In_2S_3$ bandgap is not decreased significantly when inserting vanadium. This implies again that nonradiative

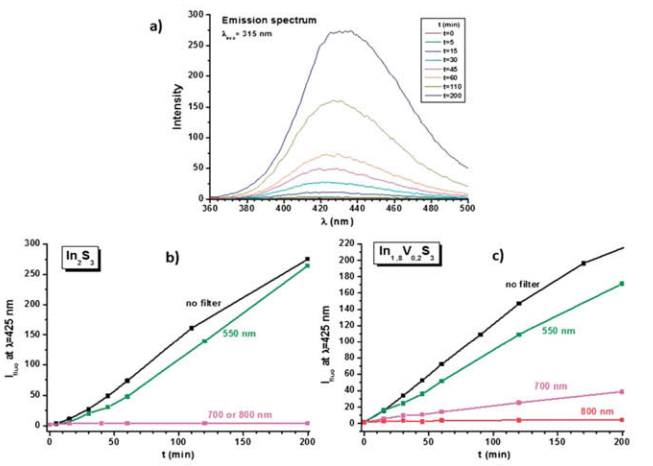


Fig. 4 a) Fluorescence observed upon exciting with 315 nm light a terephthalic acid solution which had been subjected, with $In_2S_3$ suspended in it, to irradiation during increasing times with unfiltered xenon lamp light. Time increase of the fluorescence at 425 nm measured for (b) $In_2S_3$ and (c) V:$In_2S_3$ during irradiation with different filtered wavelengths.

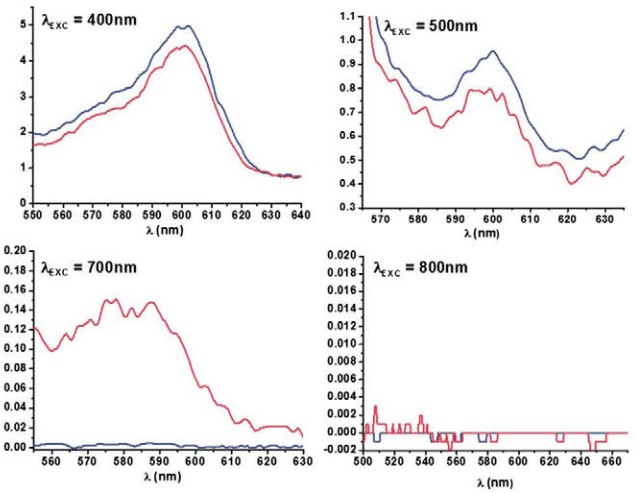


Fig. 5 Photoluminescence spectra obtained when exciting at ambient temperature the $In_2S_3$ (blue lines) and V:$In_2S_3$ (red lines) samples with different light wavelengths.

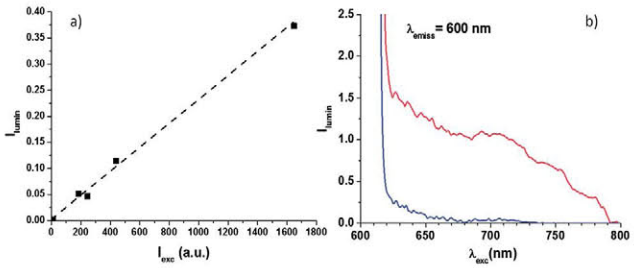


Fig. 6 Dependence of 595 nm photoluminescence intensity measured at ambient temperature for V:$In_2S_3$ on (a) intensity of exciting light at 700 nm and (b) exciting light wavelength; the latter (red line) is compared with that measured for $In_2S_3$ (blue line).

recombination is not enhanced by the presence of vanadium; as said above this is predicted by theory for concentrated dopants giving delocalized bands and agrees with experimental results.[7]

The most interesting result is that when exciting with light of wavelength ≈700 nm (photon energy ≈1.75 eV) the emission at ≈2.1 eV still appears for the V:$In_2S_3$ sample but not for the $In_2S_3$ sample. Therefore the effect of vanadium is not just causing a decrease in the bandgap. This emission is definitely absent if the excitation light wavelength is ≈800 nm (corresponding to a photon energy ≈1.55 eV). Such generation of luminescence at ≈2.1 eV when exciting with photons having energy ≈1.75 eV should not be ascribed to a mere frequency doubling due to some nonlinear optical property (as could arise, for example, from local breaking of centrosymmetric character near the vanadium dopant); in such a case the effect should be observed also when exciting with ≈1.55 eV photons. The fact that it is not so supports the interpretation that the bandgap is split asymmetrically by the V-induced IB, so that only when the incident light has energy greater than the larger of the two partial gaps (estimated to be around 1.65–1.7 eV from the results obtained here) can the two-photon cooperative process take place. Also, when changing the intensity of the exciting light, by using different monochromator slits, by a factor of up to *ca.* 8 (determined by measuring the integrated intensity of the elastically dispersed peak at the exciting wavelength), the intensity of the peak at ≈600 nm changes approximately proportionally to that intensity, and certainly not to its square (Fig. 6a). This rules out again a simple nonlinear optical effect.

We think that this observation can be ascribed to the already mentioned two-photon effect and associated with the existence of an intermediate band. Note that this ≈600 nm emission, associated with the formation of electron–hole pairs separated by the gap, behaves in a quite similar way as the photocatalytic activity shown in Fig. 3: when originated from 400 or 500 nm light its magnitude is similar in both samples; when originated from 700 nm light it is a fraction of the former one for V:$In_2S_3$ but is negligible for $In_2S_3$ and when originated from *ca.* 800 nm light it is practically null. This is appreciated more clearly in Fig. 6b, in which the emitted light detected at 595 nm is monitored as a function of the exciting wavelength. Beyond the contribution at *ca.* 600 nm due to the elastically scattered light the curves show that there is significant intensity emitted at 595 nm for the V:$In_2S_3$ sample, but not for the $In_2S_3$ sample, under excitation by photons having lower energy than the bandgap, and the range in which this is observed agrees rather well with the range in which photocatalytic activity is displayed by the former sample but not by the second one. All together, this means that the excitation produced by sub-bandgap photons can produce electrons and holes at the edges of the host semiconductor gap *via* the two-photon process, and these carriers can be practically used in electron transfers across the interface of the material, driving chemical reactions. Presumably the same charge transfer can be used to drive a photovoltaic device.

## Quantum modelling of the material

Considering our previous DFT calculations, which predict the formation of an IB within the $In_2S_3$ gap upon partial substitution of octahedral In by V,[11] the spectral response extension observed can be ascribed to the effect of such an IB. Of course, the said effective bandgap around 1.65 eV would correspond to the larger of the two sub-bandgaps involved in the IB system. Excitation across the smaller sub-bandgap could occur as well with absorption of light of longer wavelengths (as indeed observed in the spectrum), but would not give rise to photocatalytic activity since such photons cannot produce the excitation across the larger sub-bandgap which is necessary to complete the process. In contrast, the photons able to produce the larger sub-bandgap transition can of course excite also the smaller sub-bandgap transition, and can therefore sustain the two-photon process. It is noted that the ratio between sub-bandgap widths resulting from these results (*ca.* 3 : 1 or more) does not approach well the optimum one for photovoltaics (*ca.* 2 : 1); still, the material may serve to test effectively the operation of the IB PV scheme.

An additional information of interest is, whether the IB is located closer to the CB or to the VB. The experimental data described above concerning optical and photocatalytic

properties of the V:$In_2S_3$ system are compatible with both situations, but other experimental results could depend on which of these situations prevails. For example, one could try to detect spectroscopically (using fluorescent or EPR-detectable probes) which type of trapped carriers are produced upon irradiation with low energy photons which are able to excite only transitions across the smaller IB-induced sub-bandgaps. Depending on the situation one would obtain either trapped holes or trapped electrons. Quantum calculations can in principle solve the question, but standard DFT calculations such as those used by the present authors in ref. 11 and 12 do not give correct bandgaps, and are therefore not reliable enough for this purpose.

Here we try to answer this question using state-of-the-art many-body calculations, which are in principle more accurate and reliable in the prediction of bandgaps. Such calculations, if attempted with self-consistency (as indicated in the Methods part) are computationally very expensive, and carrying them out with the necessary accuracy for the 40-atom unit cell of the $In_2S_3$ structure is prohibitive for our present resources. One can, however, make use of the fact that $In_2S_3$ and $MgIn_2S_4$ are materials with very similar structures (of thiospinel type) and bandgaps (around 2.0 eV[21,40]). Also, in both of them the VB and CB are made respectively of (mainly) S (3 sp) orbitals and In (5 s) orbitals, and after partial substitution of octahedral In by V very similar band structures and density of states (DOS) curves arise in GGA level DFT calculations, as shown in ref. 11. It is thus reasonable to assume that GW-type calculations made on V-substituted $MgIn_2S_4$ (with a primitive unit cell having only 14 atoms, and therefore less costly to calculate with GW than $In_2S_3$) will give results that can be considered a good approximation to those which would be obtained with a similar calculation on the V-substituted $In_2S_3$ system.

The calculation was carried out starting with a primitive cell of $MgIn_2S_4$ with inverse spinel structure (*i.e.* the Mg atoms occupy one half of the octahedral sites and one half of the In atoms occupy all of the tetrahedral sites, giving a structure with intrinsic symmetry according to space group *Imma*), as the natural compound approaches that situation;[41] also, this inverse spinel and $In_2S_3$ coincide in having both tetrahedral and octahedral In. One of the octahedral In atoms was then substituted by V (the intrinsic symmetry decreasing then to the space group *C*2/*m*). The calculation involved computing first the electronic structure with a self-consistent COHSEX calculation, and obtaining subsequently (in non-self-consistent way) from this result the $G_0W_0$ electronic structure. All calculations were performed after a full relaxation at the LDA level of both primitive cell dimensions and atomic coordinates.

Fig. 7 shows spin-polarized densities of states (DOS) and band structures thus computed for V-substituted $MgIn_2S_4$ at the DFT–LDA, sc-COHSEX and sc-COHSEX + $G_0W_0$ levels. A partially occupied (*i.e.* crossed by the Fermi level) IB appears in all three cases in the spin-up electronic bands. The dispersion of the individual bands is also similar in all three calculations, but the position of the IB within the band gap is different. The method which can be considered more accurate (sc-COHSEX + $G_0W_0$), produces a VB maximum to IB minimum gap of 1.40 eV and an IB maximum to CB minimum gap of 0.35 eV. The energy

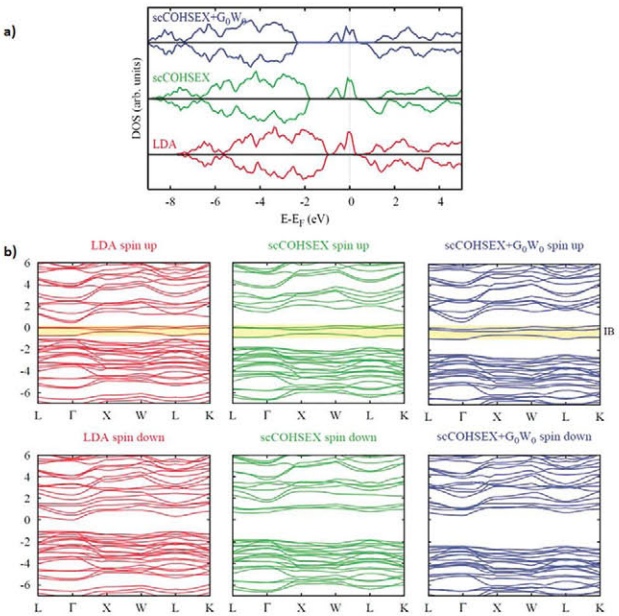


Fig. 7 Spin-polarized density of states (DOS) curves (a) and band structures (b) computed for V-substituted $MgIn_2S_4$ at the LDA, sc-COHSEX and sc-COHSEX-$G_0W_0$ levels. The vertical energy scale in (b) (in eV) is, referred to the Fermi level, taken as zero.

distance between the VB maximum and Fermi level is 2.40 eV, and from this latter to the CB minimum the distance is 0.63 eV.

It is thus noted that the overall band gap between the VB and CB predicted by this calculation is 3.03 eV, *i.e.* rather larger than the experimental bandgap found for unsubstituted $MgIn_2S_4$ (2.1–2.28 eV[40,42]), and also larger than the onset of the main absorption rise measured for the V-substituted $In_2S_3$,[12] which occurs at *ca.* 2.2 eV. It is however close to that found for unsubstituted $MgIn_2S_4$ in a similar sc-COHSEX + $G_0W_0$ calculation, which gave for it a bandgap of 3.04 eV[43] evidencing that the insertion of vanadium in the thiospinel structure does not alter much the intrinsic bandgap in agreement with the mentioned similarity in the position of the main rise in absorption occurring in the experimental optical spectrum. As said in ref. 43, the important discrepancy found for this system between the GW-type calculation (which normally reproduces bandgaps well[44,45]) and the experimental value could be due to excitonic and polaronic phenomena added to the typical effect of temperature.

In any case, given this discrepancy between the GW-computed and experimental bandgap values of the $MgIn_2S_4$ system the absolute values of the VB–IB and IB–CB gaps found here cannot be accurate. Still, we think that it is possible to infer from the results obtained here valid conclusions on the position of the IB in the present system. First of all, in all the calculations made the V-derived states form an IB partially filled and clearly separated from the VB and CB; this observation, made already in the initial DFT–GGA study of ref. 11, can thus be considered valid. Secondly, in ref. 45 the sc-COHSEX + $G_0W_0$ method performed well when predicting the bandgap of $CuGaS_2$ (the value found, 2.65 eV, was rather close to the experimental one of 2.4–2.5 eV[46]), and additional work[22] has shown that when Ga is

partially substituted by Cr in this material, leading to IB characteristics, the distance between the VB and the Cr-induced IB progressively increased when improving the theoretical approach from DFT–LDA (for which this distance was found to be smaller than the IB to CB one) through sc-COHSEX to sc-COHSEX + $G_0W_0$, so that in the latter case the VB to IB distance was larger than the IB to CB one. The same effect of the VB–IB distance increasing upon improving the theory level appeared when studying the IB features of Ti-substituted $MgIn_2S_4$.[23] We think therefore that one can give credit to the result found now, which shows a similar trend and indicates that in V-substituted $MgIn_2S_4$ (and consequently also in V-substituted $In_2S_3$) the VB to IB distance is larger than that between the IB and the CB. Consequently, the absorption onset observed at *ca.* 1.65 eV in the experimental spectrum of the V-substituted $In_2S_3$ sample[12] can be ascribed to the electron excitation across the sub-bandgap existing between the VB and the IB, which would be larger than that between the IB and the CB (as depicted in Fig. 1). The distance between this observed onset and that which can be ascribed in the same experimental spectrum to the full bandgap transition, appearing at *ca.* 2.3 eV, would correspond then to the transition between the IB and the CB. These conclusions can be relevant for further experimental studies which may be made on this system; for example, when trying to ascribe to the formation of trapped electron or hole states the effect of irradiation using photons having energy less than half of the semiconductor band gap. In addition, the results of this GW-type calculation imply that hot carriers formed by the two-photon process when using photons in the 1.7–2.0 eV range would result mainly from excitations from the IB to high energy states within the CB; *i.e.* electrons, rather than holes, would be the hotter carriers in this case. This might be relevant for the operation of any photovoltaic or photocatalytic device that was designed for the use of such hot carriers.

To complete the study, Fig. 8a presents the imaginary part of the frequency-dependent dielectric function of V-substituted $MgIn_2S_4$ in the UV-vis-NIR range, as computed from the GW result (*i.e.* at the RPA + GW level, using the sc-COHSEX + $G_0W_0$ eigenvalues), together with its separation in the contributions of the different inter-band transitions, as computed at the same level. Fig. 7b presents the resulting overall optical absorption coefficient, which is related to the $\omega\varepsilon_2$ term through multiplication by the ($\omega$-dependent) refractive index $n$, computed as well at the same theory level. Both parts of the figure include the corresponding result found for unsubstituted $MgIn_2S_4$. To obtain these latter curves it is not necessary to carry out a full optical calculation from the sc-COHSEX + $G_0W_0$ results, as in these latter curves the shape of the bands is very similar (except for the magnitude of the gap separation) to that found in the DFT–GGA calculations, so that it suffices using the bands computed with DFT–GGA and adding a scissors operator which retrieves the sc-COHSEX + $G_0W_0$ gap. It should be noted here also that the GW approach takes into account only charged excitations. Neutral excitations (*i.e.* excitonic effects) are neglected in the calculation of optical properties within this approach. However, we expect the latter to be a good approximation for intermediate-band materials, as the delocalization

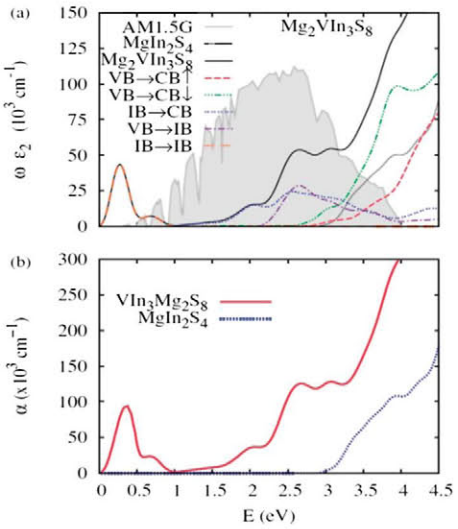


Fig. 8 (a) Imaginary part of the frequency-dependent dielectric function in the UV-vis-NIR range computed at the RPA + GW level, using the sc-COHSEX + $G_0W_0$ eigenvalues, for V-substituted $MgIn_2S_4$, together with its separation in the contributions of the different inter-band transitions. The AM1.5G solar spectrum (in arbitrary units) is plotted as well for comparison. (b) Resulting overall optical absorption coefficient. In both cases the result obtained for $MgIn_2S_4$ is included.

of the IB and its metallic character will screen the electron–hole interactions giving rise to very small or even negligible excitonic effects.

The result shown in Fig. 8b for the V-substituted system indicates, as could be expected from the results in Fig. 7, that the IB-to-VB transition starts at lower photon energy than the CB-to-IB transition. The position of these onsets, however, cannot be considered quantitatively accurate as the total bandgap is found to be overestimated. Still, it is worth noting that the amplitudes of the two absorption contributions in the sub-bandgap photon range are quite comparable, which is important since the two-photon process providing the solar efficiency improvement in the IB scheme can only be used optimally if the rates of both transitions are similar. It may also be noted in Fig. 8b that the main rise in the absorption coefficient found for the V-substituted system (at photon energies higher than those of the features observed at *ca.* 2.0 eV and below, and therefore ascribable to absorptions involving mostly the direct VB to CB transitions) appears noticeably shifted to higher energy in comparison to that found for unsubstituted $MgIn_2S_4$. This agrees with the difference in the same sense found in ref. 12 between the absorption coefficients of pure $In_2S_3$ and V:$In_2S_3$ in the range above 2.0 eV, but does not imply an increase in the VB to CB gap, as evidenced by the onset of the VB-to-CB spin up and spin down contributions to the dielectric function presented in Fig. 8a.

## Conclusions

The results presented here show that photons with energy lower than the $In_2S_3$ bandgap can be produced in this material, when

part of the In atoms in it are substituted by V atoms, electrons and holes at the CB and VB edges that can be transferred at the interface to the external medium with quite similar effectiveness as those which in non-substituted $In_2S_3$ can be generated only by photons having energy higher than its bandgap. Use of a fluorescent probe evidences that the chemical process involves OH radicals as is typical of photocatalysis in the aqueous phase. The results support the prediction made earlier that partial substitution of In by V in $In_2S_3$ produces an intermediate band (IB) of the kind that may enhance the efficiency of photovoltaic cells. Furthermore, it shows that the IB scheme can indeed operate efficiently (at least in photocatalytic processes) if implemented in a monophasic absorber of the type proposed here, in contrast with the quantum dot-based alternative which has inherently small sub-bandgap absorption coefficients.

Quantum modelling of the electronic structure of this system with a many body (GW-type) method suggests that the larger of the two sub-bandgaps in which the IB divides the intrinsic gap of the $In_2S_3$ host corresponds to the separation between the VB and the IB Fermi level, which would be about 1.65 eV; the IB Fermi level to CB separation would be then around 0.45 eV. This assignment may be relevant for further experimental mechanistic studies, using *e.g.* fluorescent probes or EPR spectroscopy, on the generation of trapped hole or electron states upon irradiation with sub-bandgap photons. The results imply also that the mentioned hot carriers correspond mainly to hot electrons, which might have practical consequences as well.

Since $In_2S_3$ is a material well known in thin film PV, making a solar cell having an absorber based on it which may serve to test the concept should be feasible. It should be noted also that for the similar system V:$MgIn_2S_4$ the absorption coefficients computed from the GW results for both sub-bandgap transitions are similar, so that these latter may occur in V:$In_2S_3$ in a well-balanced way, as is desirable, during the photon conversion process.

Finally, the wide range of light that can be used by this system in photocatalytic processes, covering the full visible spectrum, might allow a good use of this material not only in traditional disinfection and purification applications of photocatalysis but also in other solar energy harvesting schemes like those leading to photocatalytic or photoelectrochemical hydrogen generation from water. It is fortunate in this respect that the VB and CB positions in $In_2S_3$ straddle conveniently the potentials of the $H^+/H_2$ and $OH^-/O_2$ redox pairs (as also do those of $SnS_2$, the other system previously proposed by us[10] as the IB material).[47]

## Acknowledgements

This work was supported by programme NUMANCIA-2 (nr. S2009ENE-1477) from the Comunidad de Madrid. Authors thankfully acknowledge the computer resources, technical expertise and assistance provided by the Centro de Supercomputación y Visualización de Madrid (CeSViMa) and the Spanish Supercomputing Network. R. L. also thanks CSIC for an I3P PhD grant.

## Notes and references

1 M. Bosi and C. Pelosi, *Prog. Photovoltaics*, 2007, **15**, 51.
2 M. Wolf, *Proc. IRE*, 1960, **48**, 1246.
3 (*a*) A. Luque and A. Martí, *Phys. Rev. Lett.*, 1997, **78**, 5014; (*b*) A. Luque and A. Martí, *Prog. Photovoltaics*, 2001, **9**, 73.
4 S. Rehman, R. Ullah, A. M. Butt and N. D. Gohar, *J. Hazard. Mater.*, 2009, **170**, 560.
5 For a history of the evolution of the concept and a scheme of it see K. Nickelsen, *Ann. Phys.*, 2012, **524**, A157.
6 A. Martí, N. López, E. Antolín, E. Cánovas, C. Stanley, C. Farmer, L. Cuadra and A. Luque, *Thin Solid Films*, 2006, **511–512**, 638.
7 E. Antolín, A. Martí, J. Olea, D. Pastor, G. González-Díaz, I. Mártil and A. Luque, *Appl. Phys. Lett.*, 2009, **94**, 042115.
8 P. Palacios, J. J. Fernández, K. Sánchez, J. C. Conesa and P. Wahnón, *Phys. Rev. B: Condens. Matter Mater. Phys.*, 2006, **73**, 085206.
9 P. Palacios, K. Sánchez, J. C. Conesa, J. J. Fernández and P. Wahnón, *Thin Solid Films*, 2007, **515**, 6280.
10 P. Wahnón, J. C. Conesa, P. Palacios, R. Lucena, I. Aguilera, Y. Seminovski and F. Fresno, *Phys. Chem. Chem. Phys.*, 2011, **13**, 20401.
11 P. Palacios, I. Aguilera, K. Sánchez, J. C. Conesa and P. Wahnón, *Phys. Rev. Lett.*, 2008, **101**, 046403.
12 R. Lucena, I. Aguilera, P. Palacios, P. Wahnón and J. C. Conesa, *Chem. Maters.*, 2008, **20**, 5125.
13 (*a*) K. M. Yu, W. Walukiewicz, J. Wu, W. Shan, J. W. Beeman, M. A. Scarpulla, O. D. Dubon and P. Becla, *J. Appl. Phys.*, 2004, **95**, 6232; (*b*) K. M. Yu, W. Walukiewicz, J. W. Ager, D. Bour, R. Farshchi, O. D. Dubon, S. X. Li, I. D. Sharp and E. E. Haller, *Appl. Phys. Lett.*, 2006, **88**, 092110.
14 N. Ahsan, N. Miyashita, M. M. Islam, K. M. Yu, W. Walukiewicz and Y. Okada, *Appl. Phys. Lett.*, 2012, **100**, 172111.
15 S. Sonoda, *Appl. Phys. Lett.*, 2012, **100**, 202101.
16 C. H. Ho, *J. Mater. Chem.*, 2011, **21**, 10518.
17 (*a*) P. Chen, M. Qin, H. Chen, C. Yang, Y. Wang and F. Huang, *Phys. Status Solidi A*, 2013, **6**, 1098; (*b*) C. Yang, M. Qin, Y. Wang, D. Wan, F. Huang and J. Lin, *Sci. Rep.*, 2013, **3**, 1286.
18 P. Chen, H. Chen, M. Qin, C. Yang, W. Zhao, Y. Liu, W. Zhang and F. Huang, *J. Appl. Phys.*, 2013, **113**, 213509.
19 M. Dobrowolska, K. Tivakornsasithorn, X. Liu, J. K. Furdyna, M. Berciu, K. M. Yu and W. Walukiewicz, *Nat. Mater.*, 2012, **11**, 444.
20 D. L. Greenaway and R. Nitsche, *J. Phys. Chem. Solids*, 1965, **26**, 1445.
21 K. Kambas, A. Anagnostopoulos, S. Ves, B. Ploss and J. Spyridelis, *Phys. Status Solidi B*, 1985, **127**, 201.
22 I. Aguilera Bonet, PhD thesis, Universidad Politécnica de Madrid, 2010, http://oa.upm.es/3669/.
23 I. Aguilera, P. Palacios and P. Wahnón, *Phys. Rev. B: Condens. Matter Mater. Phys.*, 2011, **84**, 115106.
24 See *e.g.* (*a*) *Environmentally Benign Catalysts – Applications of Titanium Oxide-Based Photocatalysts*, ed. M. Anpo and K. V.

 

Kamat, Springer, New York, 2010; (*b*) A. Kubacka, M. Fernández-García and G. Colón, *Chem. Rev.*, 2012, **112**, 1555.

25 (*a*) W. Du, J. Zhu, S. Li and X. Qian, *Cryst. Growth Des.*, 2008, **8**, 2131; (*b*) Y. He, D. Li, G. Xiao, W. Chen, Y. Chen, M. Sun, H. Huang and X. Fu, *J. Phys. Chem. C*, 2009, **113**, 5254; (*c*) W. Wang, W. Zhu and L. Zhang, *Res. Chem. Intermed.*, 2009, **35**, 761; (*d*) X. Fu, X. Wang, Z. Chen, Z. Zhang, Z. Li, D. Y. C. Leung, L. Wu and X. Fu, *Appl. Catal., B*, 2010, **95**, 393; (*e*) R. Amutha, S. Akilandeswari, B. Ahmmad, M. Muruganandham and M. Sillanpää, *J. Nanosci. Nanotechnol.*, 2010, **10**, 8438; (*f*) G. Liu, X. Jiao, Z. Qin and D. Chen, *CrystEngComm*, 2011, **13**, 182; (*g*) S. Cingarapu, M. A. Ikenberry, D. B. Hamal, C. M. Sorensen, K. Hohn and K. J. Klabunde, *Langmuir*, 2012, **28**, 3569; (*h*) W. Wu, R. Lin, L. Shen, R. Liang, R. Yuan and L. Wu, *Catal. Commun.*, 2013, **40**, 1.

26 For a recent review, see: Z. Wang, Y. Y. Liu, B. B. Huang, Y. Dai, Z. Z. Lou, G. Wang, X. Y. Zhang and X. Y. Qin, *Phys. Chem. Chem. Phys.*, 2014, **16**, 2758.

27 See *e.g.*: M. Fernández-García, A. Martínez-Arias and J. C. Conesa, in ref. 24, pp. 277–300.

28 (*a*) S. Shen and L. Guo, *J. Solid State Chem.*, 2006, **179**, 2629; (*b*) C. Gao, J. Li, Z. Shan, F. Huang and H. Shen, *Mater. Chem. Phys.*, 2010, **122**, 183; (*c*) V. Stengl, F. Oplustil and T. Nemec, *Photochem. Photobiol.*, 2012, **88**, 265; (*d*) M.-Q. Yang, B. Weng and Y.-J. Xu, *Langmuir*, 2013, **29**, 10549; (*e*) S. Khanchandani, S. Kundu, A. Patra and A. K. Ganguli, *J. Phys. Chem. C*, 2013, **117**, 5558.

29 (*a*) X. Gonze, J.-M. Beuken, R. Caracas, F. Detraux, M. Fuchs, G.-M. Rignanese, L. Sindic, M. Verstraete, G. Zerah, F. Jollet, *et al.*, *Comput. Mater. Sci.*, 2002, **25**, 478; (*b*) X. Gonze, G.-M. Rignanese, M. Verstraete, J.-M. Beuken, Y. Pouillon, R. Caracas, F. Jollet, M. Torrent, G. Zerah, M. Mikami, *et al.*, *Z. Kristallogr.*, 2005, **220**, 558.

30 F. Bruneval, N. Vast and L. Reining, *Phys. Rev. B: Condens. Matter Mater. Phys.*, 2006, **74**, 045102.

31 M. Fuchs and M. Scheffler, *Comput. Phys. Commun.*, 1999, **119**, 67.

32 M. S. Hybertsen and S. G. Louie, *Phys. Rev. B: Condens. Matter Mater. Phys.*, 1986, **34**, 5390.

33 L. Hedin, *Phys. Rev. [Sect.] A*, 1965, **139**, 796.

34 R. W. Godby and R. J. Needs, *Phys. Rev. Lett.*, 1989, **62**, 1169.

35 T. Wolfram and S. Ellialtioglu, *Electronic and Optical Properties of d-Band Perovskites*, Cambridge University Press, Cambridge, 2006.

36 R. Lucena, F. Fresno and J. C. Conesa, *Catal. Commun.*, 2012, **20**, 1.

37 T. Charbouillot, M. Brigante, G. Mailhot, P. R. Maddigapu, C. Minero and D. Vione, *J. Photochem. Photobiol., A*, 2011, **222**, 70.

38 C. H. Ho, *J. Cryst. Growth*, 2010, **312**, 2718.

39 S. Gorai, P. Guha, D. Ganguli and S. Chaudhuri, *Mater. Chem. Phys.*, 2003, **82**, 974.

40 P. M. Sirimanne, N. Sonoyama and T. Sakata, *J. Solid State Chem.*, 2000, **154**, 476.

41 (*a*) L. Gastaldi and A. Lapiccirella, *J. Solid State Chem.*, 1979, **30**, 223; (*b*) M. Wakaki, O. Shintani, T. Ogawa and T. Arai, *Jpn. J. Appl. Phys.*, 1982, **21**, 958.

42 M. Wakaki, O. Shintani, T. Ogawa and T. Arai, *Jpn. J. Appl. Phys.*, 1980, **19**, 255.

43 M. J. Lucero, I. Aguilera, C. V. Diaconu, P. Palacios, P. Wahnón and G. E. Scuseria, *Phys. Rev. B: Condens. Matter Mater. Phys.*, 2011, **83**, 205128.

44 (*a*) M. van Schilfgaarde, T. Kotani and S. Faleev, *Phys. Rev. Lett.*, 2006, **96**, 226402; (*b*) F. Bruneval, N. Vast and L. Reining, *Phys. Rev. B: Condens. Matter Mater. Phys.*, 2006, **74**, 045102.

45 I. Aguilera, J. Vidal, P. Wahnón, L. Reining and S. Botti, *Phys. Rev. B: Condens. Matter Mater. Phys.*, 2011, **84**, 085145.

46 (*a*) J. L. Shay, B. Tell, H. M. Kasper and L. M. Schiavone, *Phys. Rev. B: Solid State*, 1972, **5**, 5003; (*b*) B. Tell, J. L. Shay and H. M. Kasper, *Phys. Rev. B: Solid State*, 1971, **4**, 2463; (*c*) J. R. Botha, M. S. Branch, P. R. Berndt, A. W. R. Leitch and J. Weber, *Thin Solid Films*, 2007, **515**, 6246.

47 Y. Xu and M. A. A. Schoonen, *Am. Mineral.*, 2000, **85**, 543.